Evolution of the $E(1/2_1^+) - E(3/2_1^+)$ energy spacing in odd-mass K, Cl, and P isotopes for $N = 20$–28

A. Gade,[1,2] B. A. Brown,[1,2] D. Bazin,[1] C. M. Campbell,[1,2] J. A. Church,[1,2] D. C. Dinca,[1,2] J. Enders,[3] T. Glasmacher,[1,2] M. Horoi,[4] Z. Hu,[1] K. W. Kemper,[5] W. F. Mueller,[1] T. Otsuka,[6,7] L. A. Riley,[8] B. T. Roeder,[5] T. Suzuki,[9] J. R. Terry,[1,2] K. L. Yurkewicz,[1,2] and H. Zwahlen[1,2]

[1]*National Superconducting Cyclotron Laboratory, Michigan State University, East Lansing, Michigan 48824, USA*
[2]*Department of Physics and Astronomy, Michigan State University, East Lansing, Michigan 48824, USA*
[3]*Institut für Kernphysik, Technische Universität Darmstadt, Darmstadt, Germany*
[4]*Department of Physics, Central Michigan University, Mount Pleasant, Michigan 48859, USA*
[5]*Department of Physics, Florida State University, Tallahassee, Florida 32306, USA*
[6]*Department of Physics and Center for Nuclear Study, University of Tokyo, Hongo, Tokyo 113-0033, Japan*
[7]*RIKEN, Hirosawa, Wako-shi, Saitama 351-0198, Japan*
[8]*Department of Physics and Astronomy, Ursinus College, Collegeville, Pennsylvania 19426, USA*
[9]*Department of Physics, Nihon University, Sakurajosui, Setagaya-ku, Tokyo 156-8550, Japan*

(Received 23 January 2006; published 15 September 2006)

The energy of the first excited state in the neutron-rich $N = 28$ nucleus ^{45}Cl has been established via in-beam γ-ray spectroscopy following proton removal. This energy value completes the systematics of the $E(1/2_1^+) - E(3/2_1^+)$ level spacing in odd-mass K, Cl, and P isotopes for $N = 20$–28. The results are discussed in the framework of shell-model calculations in the sd-fp model space. The contribution of the central, spin-orbit, and tensor components is discussed from a calculation based on a proton single-hole spectrum from G-matrix and $\pi + \rho$ meson exchange potentials. A composite model for the proton $0d_{3/2} - 1s_{1/2}$ single-particle energy shift is presented.

DOI: 10.1103/PhysRevC.74.034322 PACS number(s): 23.20.Lv, 21.60.Cs, 25.70.Mn, 27.40.+z

I. INTRODUCTION

Neutron-rich nuclei in the neighborhood of ^{44}S have attracted much attention in recent years. The question whether the high degree of collectivity observed for ^{42,44}S [1,2] is due to a breakdown of the $N = 28$ neutron-magic number or the collapse of the $Z = 16$ proton subshell gap at neutron number 28 is much discussed in the literature [3–8]. The vanishing of the $Z = 16$ subshell closure was inferred from the near-degeneracy of the proton $s_{1/2}$ and $d_{3/2}$ orbitals in the chain of K isotopes as $N = 28$ is approached [4,5,9].

Retamosa *et al.* [4] present an unrestricted shell-model calculation in a valence space including the *sd* shell for protons and the *pf* shell for neutrons. The evolution of the $E(1/2_1^+) - E(3/2_1^+)$ level spacing in the K isotopes was used to phenomenologically modify the cross-shell interaction. The authors predict the evolution of the $E(1/2_1^+) - E(3/2_1^+)$ energy difference in the $Z = 17$ and $Z = 15$ isotopic chains as neutrons fill the $f_{7/2}$ orbit. At that time, the $E(1/2_1^+) - E(3/2_1^+)$ energy splitting was neither known in any of the P isotopes with $20 \leqslant N \leqslant 28$ nor in the Cl isotopes above $N = 22$. In the present paper, we complete the systematics of the experimental $1/2_1^+ - 3/2_1^+$ level spacings in the Cl chain. The contributions of the central, spin-orbit and tensor components of the *NN* interaction to the evolution of the energy splitting are analyzed to elucidate the microscopic effects driving the changes in single-particle structure. For this, single proton-hole spectra are discussed in the framework of G-matrix and $\pi + \rho$ meson exchange potentials.

II. EXPERIMENT

The experiment was performed at the Coupled Cyclotron Facility of the National Superconducting Cyclotron Laboratory at Michigan State University. The 76.4 MeV/nucleon ^{46}Ar secondary beam was produced via projectile fragmentation of a 110 MeV/nucleon ^{48}Ca primary beam on a 376 mg/cm^2 ^{9}Be target located at the midtarget position of the A1900 fragment separator [11]. The separator was operated with 0.5% momentum acceptance and a beam purity of about 99% was achieved. The ^{46}Ar secondary beam was incident on a 191 mg/cm^2 polypropylene [$(C_3H_6)_n$] target at the target position of the S800 spectrograph [12]. The reaction products were identified event-by-event with the spectrograph's focal-plane detector system [13] in conjunction with time-of-flight information obtained from scintillators in the beam line. Figure 1 shows the particle identification for the Cl isotopes studied in this experiment. The energy-loss information from the S800 ionization chamber provides Z identification (upper panel). For a given isotope, the correlation between the dispersive angle in the S800 focal plane and the time-of-flight information resolves A (lower panel).

The magnetic rigidity of the spectrograph was centered on the inelastic scattering of ^{46}Ar off the polypropylene target (see Ref. [14]). However, the momentum acceptance of the S800 spectrograph was large enough to allow a fraction of the one-proton knockout residues ^{45}Cl and the multi-nucleon removal residues ^{43}Cl to enter the focal plane as well. Only the tail of the ^{45}Cl momentum distribution was within the acceptance, confining the present study to in-beam γ-ray spectroscopy.

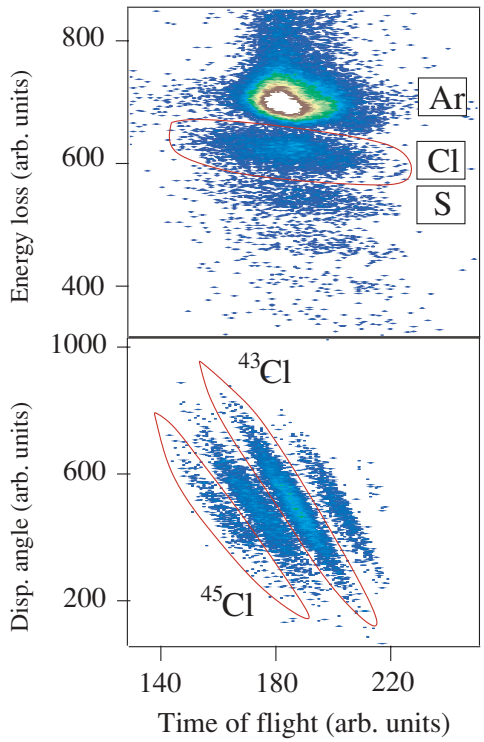

FIG. 1. (Color online) Particle identification in the S800 focal plane. The upper panel shows the energy loss measured in the ion chamber vs. time of flight taken between two scintillators. The lower panel shows for Cl isotopes the dispersive angle in the focal plane measured with the position sensitive CRDCs vs the time of flight.

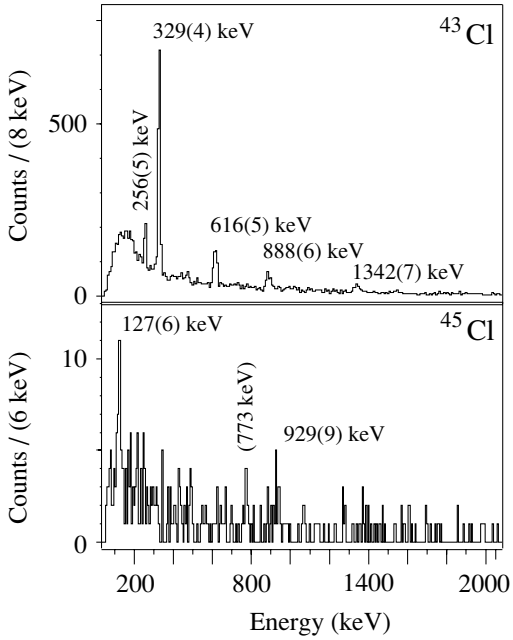

FIG. 2. Event-by-event Doppler-reconstructed γ-ray spectra in coincidence with ^{43}Cl and ^{45}Cl nucleon-removal residues produced from an ^{46}Ar secondary beam impinging on a polypropylene target.

The target was surrounded by SeGA, an array of 32-fold segmented, high-purity Ge detectors [15] arranged in two rings with angles of 90° and 37° with respect to the beam axis, respectively. 15 of the 18 SeGA detectors were used for the present experiment. The high degree of segmentation is necessary to Doppler reconstruct the γ rays emitted by the reaction residues in flight.

The upper panel of Fig. 2 shows the γ-ray spectrum detected in coincidence with ^{43}Cl produced by multinucleon removal from the ^{46}Ar secondary beam incident on the polypropylene target. The γ rays at 329(4) keV, 616(5) keV, 888(6) keV and 1342(7) keV observed in ^{43}Cl are in agreement with transitions reported in Ref. [8] from ^{48}Ca fragmentation at 60 MeV/nucleon. In addition, we see a γ-ray transition at 256(5) keV that would have been difficult to be detected by Ref. [8] due to their fairly high detection threshold for γ-ray energies (see Fig. 4 of Ref. [8] showing the γ-ray spectra of ^{43}Cl and ^{45}Cl detected with segmented Ge detectors of the Clover type following fragmentation of ^{48}Ca). The 1509(10) keV γ-ray peak observed by Sorlin *et al.* [8] might correspond to the decay of a state that is populated in the fragmentation of ^{48}Ca but unaccessible by nucleon removal of ^{46}Ar projectiles.

The lower panel of Fig. 2 displays the γ rays in coincidence with the ^{45}Cl one-proton knockout residues. The 929(9) keV γ-ray corresponds to the transition previously observed in intermediate-energy Coulomb excitation employing a NaI array for γ-ray detection [16]. The existence of a peak at 773 keV is less clear. The dominant γ-ray transition in our spectrum is found at 127(6) keV and is attributed to a transition between the $3/2^+_1$ and $1/2^+_1$ states. Shell-model calculations predict the ground state of ^{45}Cl to be $1/2^+$ with the first excited $3/2^+_1$ state at 74 keV. Our experimental result is in agreement with this expected energy splitting between the $1/2^+_1$ and $3/2^+_1$ states and completes the systematics of $E(1/2^+_1) - \bar{E}(3/2^+_1)$ in the chain of Cl isotopes for $20 \leqslant N \leqslant 28$. This 127(6) keV γ ray could not be observed by Sorlin *et al.* due to their high detection threshold (see Fig. 4 of Ref. [8]). The evolution of the energy difference in the chains of K, Cl and P isotopes for neutron numbers from $N = 20$–28 is shown in Fig. 3 and compared to shell-model calculations using the Nowacki interaction [10]. In our calculation, the protons are confined to the *sd* shell, *sd*-shell neutrons are in the closed-shell configuration $\nu(sd)^{12}$ and the remaining neutrons occupy the *fp* shell. In this space, ^{48}Ca has the configuration $\pi(sd)^{12}\nu(sd)^{12}\nu(pf)^8$. In Table I we give the *sd* shell occupation of the discussed $1/2^+_1$ and $3/2^+_1$ states in the Cl isotopes.

III. DISCUSSION

We first analyze the difference between the $d_{3/2}$ and $s_{1/2}$ proton-removal energies from Ca to K, Δ_{13}, in terms of its dependence on the interaction components. The experimental values are given in Table II. The energies of the lowest $1/2^+$ and $3/2^+$ states in ^{47}K give $\Delta_{13} = -0.36$ MeV. The centroid energy of the $s_{1/2}$ and $d_{3/2}$ strength from the ^{48}Ca$(e, e'p)^{47}$K experiment of Ref. [19] is $\Delta_{13} = -0.29$ MeV. Previous comparisons (Ref. [6] and [9]) have used a value of $\Delta_{13} =$

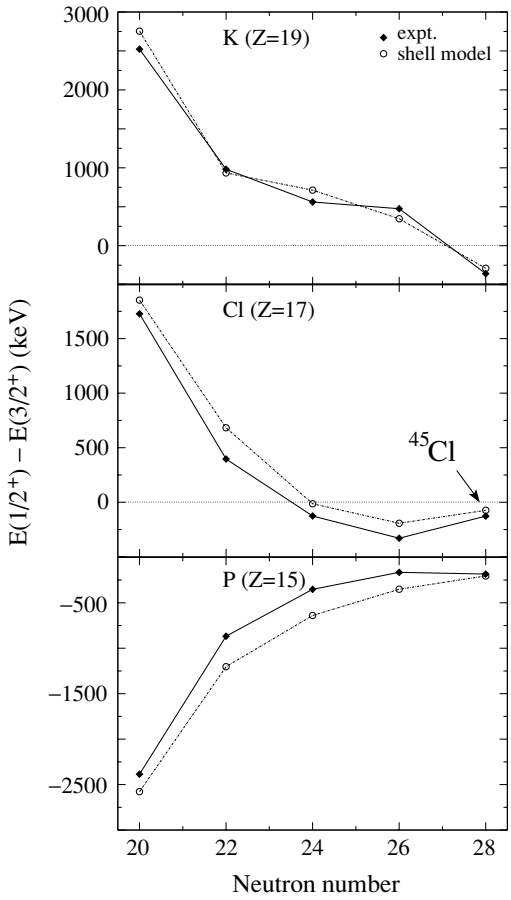

FIG. 3. Comparison of the experimental $\Delta_{13} = E(1/2_1^+) - E(3/2_1^+)$ energy splitting to shell-model calculations using the Nowacki effective interaction [10]. The ordering of the $1/2^+$ and $3/2^+$ levels in ^{41}P [17] and ^{45}Cl has not been determined by experiment and is assigned by comparison with calculations. The value for ^{43}P stems from Ref. [18], others from Refs. [8,19].

+0.29 MeV based on the older ^{48}Ca(d,^{3}He) experiment of Ref. [25]. However, the $\ell = 2$ strength reported in Ref. [25]

TABLE I. Proton shell-model occupancies n for the lowest-lying $1/2^+$ and $3/2^+$ states in chain of Cl isotopes. The rather high and constant $d_{5/2}$ occupancy is an indication of the spherical nature of these nuclei.

	J^π	$n(d_{5/2})$	$n(d_{3/2})$	$n(s_{1/2})$
^{37}Cl	$1/2^+$	5.91	2.07	1.02
	$3/2^+$	5.93	1.12	1.95
^{39}Cl	$1/2^+$	5.89	1.89	1.22
	$3/2^+$	5.89	1.31	1.80
^{41}Cl	$1/2^+$	5.86	1.90	1.24
	$3/2^+$	5.86	1.54	1.60
^{43}Cl	$1/2^+$	5.83	1.96	1.21
	$3/2^+$	5.85	1.94	1.21
^{45}Cl	$1/2^+$	5.85	2.22	0.93
	$3/2^+$	5.91	2.36	0.73

TABLE II. Splitting between the $d_{3/2}$ and $s_{1/2}$ proton hole energies Δ_{13} in units of MeV. The result for the G-matrix calculation is decomposed into the central, spin-orbit and tensor contribution.

Δ_{13} (MeV)	^{39}K	^{47}K	^{39}K − ^{47}K
"expt."[a]	2.52	−0.36	2.88
shell model[b]	2.75	−0.31	3.06
G-matrix total	3.66	−0.73	4.39
(central)	0.98	−1.28	2.26
(spin-orbit)	2.68	2.10	0.58
(tensor)	0.00	−1.55	1.55
$\pi + \rho$ tensor [9]	0.00	−1.67	1.67

[a] $E(1/2_1^+) - E(3/2_1^+)$.
[b] With the Nowacki effective interaction [10].

could be either attributed to $d_{3/2}$ or $d_{5/2}$ and it was simply assumed that all states except the ground state were of spin and parity $5/2^+$. In Ref. [19] the value of −0.29 is based on new J^π assignments given in Table I of that paper, but it is not clear to us if these assignments are firm. In the shell-model calculations the lowest energy-spacing is −0.31 MeV compared to the centroid energy spacing of −0.17 MeV.

In order to have a microscopic interpretation of the results we have calculated the single-hole spectrum for protons from a G-matrix potential [20] based on the Paris NN potential. The results are given in Table II broken down into the contributions of the central, spin-orbit and tensor components of the interaction. It has been shown that the monopole part of the G matrix is not so reliable [21–23]; therefore, it is of interest how the individual contributions compare to other calculations. The importance of the spin-isospin part of the NN interaction has been pointed out in Ref. [24] for the changes of the shell structure across the nuclear chart. It is worth mentioning that the monopole part of the tensor force has been shown in Ref. [9] to change the shell structure in a unique and robust way across the nuclear chart. Table II shows the effect of the tensor part of the present G-matrix calculation and the tensor contribution as derived from the one-π and one-ρ meson exchange tensor potential similar to Ref. [9] for $A = 40$. One notices that the two tensor results are remarkably close to each other. This is in fact an example of the universality of the tensor monopole effect from its longer range part as pointed out in Ref. [9].

The tensor part can be further examined by the $d_{5/2} - d_{3/2}$ spin-orbit splitting, Δ_{53}, as shown in Table III. The experimental energy is the energy centroid of the $d_{5/2}$ hole strength observed in ^{40}Ca [25] and ^{48}Ca [19]. The Nowacki interaction results are again based on the $(f_{7/2})^8$ neutron configuration. (The centroid energy from the full pf-shell model space is 5.76 MeV.) One observes a decrease in the experimental spin-orbit interaction that, when compared to the G-matrix calculation, is mainly attributed to the tensor interaction, consistent with Ref. [9]. In fact, Table III indicates that the result of the one-π and one-ρ meson exchange tensor potential is in very good agreement with the experiment.

TABLE III. Splitting between the $d_{5/2}$ and $d_{3/2}$ proton hole energies Δ_{53} in units of MeV. The result for the G matrix is decomposed into the central, spin-orbit and tensor contribution.

Δ_{53} (MeV)	^{39}K	^{47}K	^{39}K $-$ ^{47}K
"expt."[a]	7.5	4.8	2.7
shell model[b]	7.4	5.92	1.48
G matrix total	3.94	0.84	3.10
(central)	0.00	−0.32	0.32
(spin-orbit)	3.94	3.86	0.08
(tensor)	0.00	−2.70	2.70
$\pi + \rho$ tensor [9]	0.00	−2.78	2.78

[a]Energy centroids from Refs. [19,25].
[b]With the Nowacki effective interaction Ref. [10].

The absolute spin-orbit interaction obtained with the G-matrix interaction in ^{40}Ca amounts only for about 60% of the experimental value (first column of Table III). It has been shown that the spin-orbit splitting can be reproduced by a microscopic calculation based on the UMOA method from the bare NN interaction for ^{16}O [26]. In this calculation, more complex components are included but their effects are renormalized in the conventional shell-model picture. The three-body interaction has been shown also to contribute to the spin-orbit splitting in light nuclei [27]. Thus, contrary to the tensor force, the relation between the spin-orbit force and the splitting remains to be clarified.

The Skyrme Hartree-Fock (HF) method can also be used to calculate the central interaction contribution to Δ_{13} (this is done by calculating the single-particle spectrum with the Skyrme spin-orbit strength set to zero). The values from the Skyrme SKX [28] HF calculation are given in the second row of Table IV. The Skyrme results can differ from the G-matrix values due to finite well and density-dependent (or implicit effective three-body) effects. However, this HF does not include the tensor contribution.

Taking all of these into account we might make a composite model of the single-particle shifts based on HF for central, G-matrix for spin-orbit (Table II) and $\pi + \rho$ for tensor contributions. The results as given in Table IV are in reasonable agreement with experiment when the spin-orbit part from the G matrix is scaled by a factor of 1.9 as obtained from Table III. The need for rescaling the spin-orbit part is mainly due to monopole effects only inaccurately taken into account. We note that the monopole effect from the central potential differs considerably between the G-matrix and SKX interactions, which implies intrinsic theoretical difficulties. The relative importance of the central and spin-orbit potentials cannot be clarified in the present study, however, their combined effect seems to be about half of the tensor monopole effect for Δ_{13}, while negligible for Δ_{53}. A more precise evaluation of their magnitude and interplay remains an intriguing problem. The $1/2^+$ proton (Nilsson) state, which is the highest $K = 1/2^+$ of sd-shell origin, can be pushed up due to deformation. This would result in a lower energy of the $1/2^+$ level in the observed spectrum of the actual nucleus. This could occur more easily as $d_{3/2}$ and $s_{1/2}$ come closer in energy (i.e., stronger mixing). Thus, in this case, the "experimental" Δ_{13} would appear larger than the pure single-particle effect. This point should be taken into consideration more precisely in the future.

TABLE IV. Splitting between the $d_{3/2}$ and $s_{1/2}$ proton hole energies Δ_{13} in units of MeV compared to a composite model of the single-particle shifts. The central part is obtained from the SKX Skyrme HF calculation, the spin-orbit part is taken from the G-matrix approach of Table II and the tensor contribution is based on the $\pi + \rho$ potential [9]. The spin-orbit contribution is scaled by a factor of 1.9 obtained from Table III.

Δ_{13} (MeV)	^{39}K	^{47}K	^{39}K $-$ ^{47}K
"expt."[a]	2.52	−0.36	2.88
total	3.00	−0.43	3.43
(Skyrme central)	−2.09	−2.75	0.66
(1.9 × G-matrix spin-orbit)	5.09	3.99	1.10
($\pi + \rho$ tensor)	0.00	−1.67	1.67

[a]$E(1/2_1^+) - E(3/2_1^+)$.

IV. SUMMARY

In summary, we report on the first determination of the $|E(1/2_1^+) - E(3/2_1^+)| = 127(6)$ keV energy splitting in the $N = 28$ nucleus ^{45}Cl observed following the one-proton removal from a ^{46}Ar secondary beam upon collision with a polypropylene target. The evolution of the energy splitting is compared to shell-model calculations in the sd-fp model space. Its dependence on the interaction components, central, spin-orbit and tensor, is discussed for the chain of K isotopes from calculations based on the G-matrix and $\pi + \rho$ tensor potential. A similar analysis is performed for the splitting between the $d_{5/2}$ and the $d_{3/2}$ orbit where the experimental determination of the location of the $d_{5/2}$ single-particle strength in P and Cl has to remain a challenge for future experiments. The tensor monopole effect is seen as almost the sole source of the change of the $d_{5/2} - d_{3/2}$ spin-orbit splitting, while the central potential shows a certain effect for the change of the $s_{1/2} - d_{3/2}$ spin-orbit splitting. The change of the $1/2^+ - 3/2^+$ splitting contains more uncertainties in relation to single-particle properties and needs further studies. In this respect, the present experiment can be a first step towards a more comprehensive understanding of this region.

ACKNOWLEDGMENTS

Valuable discussions with F. Nowacki are acknowledged. We thank A. Stolz, T. Ginter, M. Steiner and the NSCL cyclotron operations group for providing the high-quality secondary and primary beams. This work was supported by the National Science Foundation under Grants No. PHY-0110253 and PHY-0244453. This work was supported in part by a Grant-in-Aid for Specially Promoted Research (No. 13002001) from the MEXT.

[1] H. Scheit *et al*., Phys. Rev. Lett. **77**, 3967 (1996).
[2] T. Glasmacher *et al*., Phys. Lett. **B395**, 163 (1997).
[3] T. R. Werner *et al*., Phys. Lett. **B335**, 259 (1994).
[4] J. Retamosa, E. Caurier, F. Nowacki, and A. Poves, Phys. Rev. C **55**, 1266 (1997).
[5] P. D. Cottle and K. W. Kemper, Phys. Rev. C **58**, 3761 (1998).
[6] P. D. Cottle and K. W. Kemper, Phys. Rev. C **66**, 061301(R) (2002).
[7] D. Sohler *et al*., Phys. Rev. C **66**, 054302 (2002).
[8] O. Sorlin *et al*., Eur. Phys. J. A **22**, 173 (2004).
[9] T. Otsuka, T. Suzuki, R. Fujimoto, H. Grawe, and Y. Akaishi, Phys. Rev. Lett. **95**, 232502 (2005).
[10] S. Nummela *et al*., Phys. Rev. C **63**, 044316 (2001).
[11] D. J. Morrissey *et al*., Nucl. Instrum. Methods Phys. Res. B **204**, 90 (2003).
[12] D. Bazin *et al*., Nucl. Instrum. Methods Phys. Res. B **204**, 629 (2003).
[13] J. Yurkon *et al*., Nucl. Instrum. Methods Phys. Res. A **422**, 291 (1999).
[14] L. A. Riley *et al*., Phys. Rev. C **72**, 024311 (2005).
[15] W. F. Mueller *et al*., Nucl. Instrum. Methods A **466**, 492 (2001).
[16] R. W. Ibbotson, T. Glasmacher, P. F. Mantica, and H. Scheit, Phys. Rev. C **59**, 642 (1999).
[17] C. M. Campbell, Ph.D. thesis, Michigan State University, in preparation.
[18] J. Fridmann *et al*., Nature (London) **435**, 922 (2005).
[19] G. J. Kramer, H. P. Blok, and L. Lapikas, Nucl. Phys. **A679**, 267 (2001).
[20] A. Hosaka, K. I. Kubo, and H. Toki, Nucl. Phys. **A444**, 76 (1985).
[21] J. B. McGrory, B. H. Wildenthal, and E. C. Halbert, Phys. Rev. C **2**, 186 (1970).
[22] A. Poves and A. P. Zuker, Phys. Rep. **70**, 235 (1981).
[23] B. A. Brown and B. H. Wildenthal, Annu. Rev. Nucl. Part. Sci. **38**, 29 (1988).
[24] T. Otsuka, R. Fujimoto, Y. Utsuno, B. A. Brown, M. Honma, and T. Mizusaki, Phys. Rev. Lett. **87**, 082502 (2001).
[25] P. Doll, G. J. Wagner, K. T. Knopfle, and G. Mairle, Nucl. Phys. **A263**, 210 (1976).
[26] S. Fujii, R. Okamoto, and K. Suzuki, Phys. Rev. C **69**, 034328 (2004).
[27] P. Navratil and E. W. Ormand, Phys. Rev. C **68**, 034305 (2003).
[28] B. A. Brown, Phys. Rev. C **58**, 220 (1998).